25. STABLE ISOTOPES ($^{18}O/^{16}O$) AND $^{87}Sr/^{86}Sr$ RATIOS IN PORE FLUIDS OF THE CHILE TRIPLE JUNCTION ACCRETIONARY PRISM: IMPLICATIONS FOR DIAGENESIS AND FLUID MIGRATION[1]

Yan Zheng,[2] Philip N. Froelich,[2] Marta E. Torres,[3] and Aline N. Dia[4]

ABSTRACT

Oxygen and strontium isotopic composition of sedimentary pore fluids obtained by drilling at the Chile Triple Junction have been used to obtain information on the diagenesis and transport mechanisms of fluids. Samples were collected from three sites located on an east–west transect of the pre-collision zone (Sites 859, 860, and 861) and from Site 863 located at the base of the trench slope at the point where the Chile Ridge is being subducted.

Closer to the toe of the wedge (Sites 859 and 860), non-steady state depth profiles were obtained, whereas linear chemical and isotopic profiles at the upper trench slope (Site 861) are indicative of diffusion of solutes at this site. The nature of fluids from the sites located in the transect prior to ridge subduction is quite different from that observed after ridge subduction (Site 863). Even though in all cases oxygen and strontium isotopic fingerprint indicates alteration of volcanogenic sequences to form authigenic clay mineral, the reactions that modified the chemical composition at Sites 859, 860, and 861 occurred at low temperatures, while high temperature reactions are responsible for the isotopic composition of the fluids at Site 863. At this later site, the ^{18}O of pore fluids show values as high as 0.7‰ SMOW and a $^{87}Sr/^{86}Sr$ ratio as low as 0.706 in the interval from 400 to 500 mbsf, a sediment section characterized by the presence of a cementation front and steep chemical gradients in the pore fluids. These data suggest that the basal fluids (>400 mbsf) at this site are likely to have been influenced by the hydrothermal reactions occurring at high temperatures.

INTRODUCTION

Circulation of pore fluids has a significant effect on the transport of chemical constituents and heat in virtually all crustal processes (Langseth, 1988; Taylor, 1990). In accretionary prisms, materials off-scraped from the subducting oceanic lithosphere promote fluid-rock interactions in a dynamic structural environment (von Huene and Scholl, 1991). Previous studies of several accretionary prisms (Han and Suess, 1989; Gieskes et al., 1989; Vrolijk et al., 1990; Kastner et al., 1990, 1992; Martin, 1992; Yamano et al., 1992) have documented subduction-induced migration and expulsion of fluids through studies of the chemical and isotopic compositions of the dissolved constituents in pore water. The chemical composition changes due to diagenesis are easier to detect in fluid phase than in the authigenic secondary phases. Therefore, fluid sources and processes associated with fluid-rock interaction can often be identified. Changes in the composition (i.e., Ca, Mg, ^{18}O, and $^{87}Sr/^{86}Sr$) of the fluids have been observed in Ocean Drilling Program (ODP) sites (Vrolijk et al., 1990; Kastner et al., 1992; Martin, 1992) and their systematics are understood well enough to be used as tracers of the migrating fluids.

The oxygen isotopic composition of the pore fluids are especially useful simply because oxygen is abundant in both solid and fluid phases and ^{18}O has distinct signatures upon rock-fluid alteration. Major chemical changes are necessary to produce significant shifts in ^{18}O. In contrast, minor mineralogical changes can produce large changes in the chemical composition of the pore fluid. Because of the temperature dependence of the fractionation factor between authigenic mineral and water (α_{m-w}), fluid-rock reactions can cause depletion or enrichment of ^{18}O of the pore fluids (Lawrence, 1990). A summary of the changes in oxygen and hydrogen isotopic compositions from fluid-rock interactions is available in Kastner et al. (1991).

In general, because α_{m-w} approaches unity with increasing temperature, 18O of pore fluid will approach that of the secondary mineral product and appear to be ^{18}O-enriched relative to seawater. Conversely, because α_{m-w} is much larger than one at low temperature, ^{18}O of pore fluid will deviate from that of the secondary mineral product and appear to be ^{18}O-depleted relative to seawater.

Examination of the isotopic composition of dissolved strontium can help constrain the sources and flow paths of fluids. Fluids containing $^{87}Sr/^{86}Sr$ ratio more radiogenic than seawater probably originate from interactions with continental crust. On the other hand, less radiogenic $^{87}Sr/^{86}Sr$ ratio indicates fluids that have interacted with oceanic basement (Kastner et al., 1992). This information is of critical significance because drilling in this accretionary wedge transect did not reach basement at any of the sites. In addition, $^{87}Sr/^{86}Sr$ ratios of the pore fluids have been widely used as very sensitive indicators of diagenetic reactions involving alteration of volcanic matter dispersed in sediments and recrystallization of carbonates (Elderfield and Gieskes, 1982).

The results of interstitial water ^{18}O and $^{87}Sr/^{86}Sr$ ratio depth profiles from four sites of ODP Leg 141 (accretionary prism of Chile Triple Junction) are reported here. We have utilized these ^{18}O and $^{87}Sr/^{86}Sr$ ratio data to infer the possible origins and pathways of fluid migration in this complex geological environment characterized by the subduction of an active ridge crest.

TECTONIC SETTINGS

The Chile Margin Triple Junction represents the only presently active ridge-trench-continent collision where the overriding plate is composed of continental lithosphere. Reconstruction of plate motions and continental margin geology show that the Chile Ridge first collided with the Chile Trench about 14 Ma (Cande et al., 1987). Due to the simple plate geometry of the collision, it is possible to observe what happens before, during, and after a ridge-trench collision by studying the geology north, adjacent to, and south of the triple junction.

Three sites (859, 860, and 861) were drilled on the east–west transect in the pre-ridge collision zone on multichannel seismic (MCS) reflection Line 745, and one site (Site 863) was drilled on top of the subducting ridge axis on MCS Line 751 (Bangs et al., 1992).

Line 745 is located where the ridge is expected to collide with the lower trench in approximately 100 ka. The margin prior to ridge collision is characterized by a small accretionary complex and forearc basin that lies along the lower trench slopes (Fig. 1). Tectonic interaction of the ridge with the margin is minimal at this stage. The décollement thrust between the descending plate and the overlying accretionary complex is not clearly imaged on Line 745.

At Line 751 the ridge was subducted approximately 50 ka. Tectonic interaction of the ridge is more pronounced (Fig. 2). The toe of the small accretionary complex appears to have collapsed as the east wall of the ridge axis passed beneath the lower trench slope and to have filled part of the large bathymetric depressions of the ridge axis. Thrust sequences of the accretionary complex cannot be identified, presumably due to the intensive deformation of the wedge. The recovered section (Site 863) was tilted vertically, presumably upon collision.

METHODS AND SAMPLE HANDLING

Pore fluids were separated from sediments aboard ship by multiple squeezing with titanium squeezers and filtered prior to storage. Unfortunately, the total depths of all drill sites did not penetrate either the décollement or the oceanic basement, preventing direct investigation and sampling of processes at depth. The ^{18}O analyses were determined from 2.2 ml of pore fluids (stored sealed in glass ampoules) at Lamont-Doherty Earth Observatory by equilibrating CO_2 with the water samples at 35°C (Fairbanks, 1982), and analyzing the $^{18}O_{CO_2}$ with a gas mass spectrometer (MAT 251). The results are reported relative to SMOW with errors of 0.06‰ (2σ) based on seven replicates of NADW. Analysis of lab standard NADW over the course of the study yielded a mean value of -1.15 ± 0.03‰. Samples for $^{87}Sr/^{86}Sr$ ratio analysis were prepared and analyzed in the Laboratoire de Géochimie et Cosmochimie in Paris. The measured ratios were normalized to $^{86}Sr/^{88}Sr$ of 0.1194. A mean value of 0.710259 ± 26 was obtained for 25 analyses of the NBS SRM 987 standard. Analyses of seawater standard (IAPSO) over the course of the study yielded a mean value of 0.709192 ± 13. All shorebased measurements are summarized in Table 1.

RESULTS AND DISCUSSION

Accretionary Prism—Pre-ridge Collision Zone

Site 861

Drilling at Site 861 penetrated and sampled Pleistocene to late Pliocene forearc basin strata in the middle trench slope. The sediment is of glacial-marine origin, with a component of volcanic-arc and crystalline basement materials. The underlying basement is continental (Behrmann, Lewis, Musgrave, et al., 1992).

Linear gradients of ^{18}O, $^{87}Sr/^{86}Sr$ and major cations in the samples from Site 861 indicate no advection of fluids between the seafloor and 350 mbsf (Fig. 1; Behrmann, Lewis, Musgrave, et al., 1992). The high value ^{18}O at the top of sediment column (16.95 mbsf) could be due to the downward diffusion of heavier glacial bottom water (Schrag and DePaolo, 1993), likely to be about 1 to 1.2‰ heavier than present (about -0.05‰). The large negative shift of ^{18}O and non-radiogenic $^{87}Sr/^{86}Sr$ both indicate low-temperature alteration of basalt or volcanic ash.

A decrease in pore fluid ^{18}O with depth is commonly observed in accretionary prisms (Vrolijk et al., 1990; Kastner et al., 1992; Martin et al., 1992). Because volcanic ash and continental detritus are abundant at Site 861, we attribute this decrease to conversion of volcanic ash to authigenic clay minerals, mainly smectites. Correlation between the ^{18}O and Cl, Na concentrations (Fig. 3) supports this scenario because Cl and Na must increase as water is consumed. Also, positive correlation between Mg and ^{18}O (Fig. 3) is consistent with the formation of Mg-rich smectites.

Material balance considerations of the predicted mass of igneous reactants converted at Site 861 are reasonable. Porosity decreases

from 70% at the top of the hole to about 40% at the bottom. The thermal gradient below 20 m is 56°C/km. The average ^{18}O of pore fluid is -1.38‰. These characteristics are similar to those observed at DSDP Site 323 (Lawrence et al., 1979). Using an analogy to that of DSDP Site 323, we estimate the thickness of the reaction zone at Site 861 to be 40 m of volcanic ash, or 20 m of basalt, or 65 m of continental detritus in a closed system. If diffusive ^{18}O influx is included to balance reaction loss, at most a factor of 2 or so must be added to the above estimates.

Although the linear gradients at Site 861 suggest that there is no advective flow between the seafloor and 350 mbsf, we cannot assume that the alteration of volcanic components only takes place below 300 m because to achieve the observed linear gradient as observed, the diffusion relaxation time is more than 10 Ma. The age of the sediment at Site 861 is less than 2 to 3 Ma. Alteration during burial must contribute to the gradient; and thus it remains enigmatic how this linear gradient was achieved.

The gradient change at 350 mbsf corresponds to the transition from lithologic Unit II to Unit III and might be explained as a diagenetic front if further evidence of mineralogical changes in solid phases can be identified. However, since no discontinuities were observed in the other major chemical fluid compositions (Behrmann, Lewis, Musgrave, et al., 1992), it is more likely that the positive deviation of ^{18}O from the expected linear gradient is due to an artifact in the sample processing. Pore fluid may have evaporated during the long time interval needed to squeeze the fluid out of these low porosity sediments. At 20°C, evaporated water vapor is about 9‰ lighter than the bulk liquid. Evaporation of 5% of the sample could shift ^{18}O about $+0.5$‰, sufficient to cause the deviation.

In summary, isotopic and geochemical evidence does not support vigorous lateral fluid movement in the upper 350 m of Site 861. No gas-hydrates are inferred to be present from the isotopic data, nor from the pore fluid chemical composition.

Sites 859 and 860

Site 859 was drilled at the toe of an approximately 10-km-wide wedge at the leading edge of the accretionary prism. Drilling at Site 860 penetrated and sampled the seaward flank of a forearc basin and the underlying accretionary wedge. The oldest ages recovered at both sites are Late Pliocene.

At both sites, distinct non-steady state nature of the ^{18}O, $^{87}Sr/^{86}Sr$ ratio, major cations, Cl and Si are observed (Fig. 1; Behrmann, Lewis, Musgrave, et al., 1992). The ^{18}O is depleted compared to seawater, while Ca concentration increases and Mg concentration decreases with depth. Alteration of volcanic ash or basalt can be invoked to explain the ^{18}O depletion and non-radiogenic $^{87}Sr/^{86}Sr$ ratio. However, Ca and Mg concentration vs. ^{18}O do not display linear correlations. The discontinuities seen in the pore fluid depth profiles must be due to either diagenetic fronts or to exotic fluid flow.

Site 859

A prominent discontinuity in the degree of lithification was found between 216 and 235 mbsf. In addition, the temperature profile is extremely nonlinear and suggests recent lateral movement of both cool and hot fluids through a narrow region of the wedge. The ^{18}O profile has a minimum of ^{18}O equal to -3.8‰ at 219 mbsf and the $^{87}Sr/^{86}Sr$ ratio reaches 0.70623 at 257 mbsf (Fig. 1). Discontinuities of Ca, Mg, K, Sr, Li, and Si are also observed at this depth (Behrmann, Lewis, Musgrave, et al., 1992).

There are two possible scenarios to explain these observations. First, there could be injection of fluids along the lithological transition zone, likely originating from an external source where alteration of volcanic reactants is more complete (more depleted ^{18}O and very nonradiogenic $^{87}Sr/^{86}Sr$ ratio). While low $^{87}Sr/^{86}Sr$ ratios suggest that pore fluids have almost certainly been influenced by fresh basalt, the negative shift of ^{18}O requires the alteration must be low-temperature

Table 1. Isotopic data for CTJ.

Core, section, interval (cm)	Depth (mbsf)	18O SMOW (MS)	87Sr/86Sr (TIMS)	Si μM* (Spec)		Core, section, interval (cm)	Depth (mbsf)	18O SMOW (MS)	87Sr/86Sr (TIMS)	Si μM* (Spec)
141-859A-						141-861D-				
3H-3, 145–150	15.15	–0.51	0.70831			7R-02, 125–135	402.85	–2.60		
11X-2, 140–150	71.20		0.70715			15R-01, 0–10	476.30	–2.71		
13X-1, 100–110	79.00	–2.35				141-863A-				
14X-2, 140–150	90.42	–2.11	0.70722			1H-03, 145-150	4.45	–0.13		
141-859B-						2H-03, 145–150	13.05		0.70916	
1R-2, 145–150	54.95	–1.40				3H-03, 145–150	22.55	–0.13		
4R-1, 140–150	141.40	–3.10				5H-01, 45–150	38.55	–0.17		
10R-3, 0–10	199.70		0.70646			6H-01, 140–150	48.00		0.70911	
12R-3, 96–106	219.26	–3.76				7X-03, 140–150	60.50	–0.11		
16R-2, 140–50	257.50	–2.58	0.70623			8X-02, 140–150	68.40		0.70837	
25R-3, 140–150	345.60	–2.25	0.70728			9X-01, 65–75	76.05	0.08	0.70837	
32R-1, 90–100	409.50	–2.15	0.70733			19X-01, 57–65	172.60	–0.13		
141-860B-						21X-01, 45–50	191.70		0.70913	
2H-3, 145–150	5.90		0.70916			23X-CC, 25–30	210.80	–0.15		
3H-3, 145–150	15.40	–0.31				25X-0, 43–53	230.20	–0.19		
4H-3, 145–150	24.90		0.70894			26X-01, 64–74	240.10		0.70896	
5H-2, 140–150	32.80	–0.90				27X-01, 82–92	250.20	–0.09		
7H-4, 140–150	54.80	–1.46	0.70988			29X-01, 70–80	269.10	0.03		
14X-1, 140–150	100.50	–1.90				31X-CC, 15–20	288.40	–0.04	0.70897	
15X-2, 140–150	110.10		0.70883			141-863B-				
16X-2, 140–150	119.70	–2.67				4X-03, 140–150	330.30	0.05		
19X-4, 140–150	143.00	–2.60				8N-01, 79–89	358.20	–0.02		
20X-2, 0–10	147.30					11R-01, 11–18	376.70	0.06		
21X-1, 124–134	156.70	–2.27				13R-01, 20–30	396.00	0.12		
24X-1, 140–150	185.80	–2.31				15R-01, 140–150	416.60	0.36	0.70704	
25X-1, 140–150	195.50		0.70861			19R-02, 140–150	456.60	0.60		
29X-1, 140–150	234.20	–2.03				21R-01, 96–108	474.00	0.39		
33X-1, 130–145	272.50	–2.40				22R-03, 90–100	486.30		0.70665	
34X-3, 0–15	283.80		0.70875			23R-03, 140–150	496.80	0.68		
43X-1, 85–100	360.00	–2.09				25R-02, 140–150	514.60	0.61		
64X-2, 40–50	552.10	–2.75	0.70843			27R-3, 140–150	535.00	0.62	0.70615	
141-861C-						31R-03, 140–150	573.50			155
3H-3, 145–150	16.95	0.18	0.70912			32R-05, 140–150	586.20	0.52		157
4H-5, 145–150	26.45					33R-01, 105–115	589.40			152
5H-5, 145–150	37.75		0.70905			34R-03, 140–150	602.50		0.70609	155
12X-1, 140–150	91.50	–0.41	0.70897			35R-03, 138–148	612.10			135
15X-3, 140–150	123.40	–0.60	0.70891			36R-03, 140–150	621.30	0.49		144
18X-3, 140–150	152.90	–0.84				37R-04, 140–150	632.90			172
21X-1, 140–150	171.60	–1.00				38R-02, 140–150	639.50			146
25X-4, 140–150	214.80	–1.30				39R-01, 125–140	647.50	0.42		
27X-3, 80–90	223.41		0.70881			40R-01, 110–120	657.00		0.70624	131
32X-1, 60–70	257.60	–1.65				44R-02, 137–147	697.30			144
36X-2, 140–150	298.50	–1.99				49R-03, 135–150	737.50		0.70633	117
39X-2, 52–62	326.22	–2.28								

Note: * = shorebased Si data.

(<200°C). Second, bedding-parallel faulting of sediments between 216 and 235 mbsf may have caused discontinuities in the chemical and isotopic compositions across the fault, in which case the chemical depth profiles were initially different above and below the fault. Diffusion after faulting will act to smooth the discontinuities with time. Unfortunately, only one sample is located within the transition zone, so that it is difficult to determine which scenario is correct. Nevertheless, the evidence is consistent with a very dynamic environment–strong deformation and fluid migration.

Although a dramatic decrease of Na and Cl between 30 and 70 mbsf was attributed to drilling-induced dissociation of gas-hydrate occupying <25% of the pore space (Froelich et al., this volume), it is not seen in the 18O data. At the Middle America margin off Guatemala, pore-fluid-freshening (salinity of 16‰) due to gas-hydrate decomposition was accompanied by an 18O enrichment of up to 2.6‰ (Hesse and Harrison, 1981).

Site 860

Although similar to Site 859, this site is located further landward in the middle of the trench slope. Here a discontinuity in 18O at 110 to 140 mbsf, with a 18O minimum of –2.7‰ (Fig. 1), suggests mechanisms similar to Site 859. However, much less change of 87Sr/86Sr ratio is observed, indicating low-temperature alteration from altered basalt or volcanic ash. At 55 mbsf, 87Sr/86Sr ratio is higher than the seawater value, suggesting perhaps alteration continental detritus. Since no WSTP temperatures were measured below 60 m, an exotic water input explanation is less convincing. Nevertheless, one appar-

ently reliable ADARA measurement at 130 mbsf suggests that the thermal gradient decreases to 30°C/km at depth, while in the upper 70 m it is about 140°C/km. This may imply a thermal gradient change induced by fluid flow.

Accretionary Prism After Ridge-Trench Collision

Site 863

Site 863 (Fig. 2) is located at the foot of the trench wall about 5 km landward of the toe, directly above the subducted Chile Ridge spreading center. Total depth (743 mbsf) did not penetrate the décollement nor oceanic basement (~1400 mbsf). From 250 mbsf to total depth, this turbidite trench deposit, originally accreted to the trench slope, was tilted upon collision with the ridge crest some 20 to 50 ka ago (Behrmann, Lewis, Musgrave, et al., 1992). The bedding attitude is nearly vertical so the silt-sandstone could provide a vertical conduit for periodic fluid migration from depth, and leave hydrothermal imprints on the overriding plate and accretionary prism. The deformation of sediments and chemical composition of rocks, pore fluids and gases were expected to display the effects of ridge subduction.

A very unique pore fluid 18O profile is observed (Fig. 2). The entire section has 18O values close to or higher than seawater, with a 18O maximum of 0.7‰ at 500 mbsf. The non-steady state 18O and chemistry profiles (Behrmann, Lewis, Musgrave, et al., 1992) imply that fluid composition is not simply controlled by upward diffusion.

Dissociation of gas-hydrates is unlikely to be the reason for pore water 18O enrichment at Site 863 because gas-hydrate is not thermodynamically stable at these depths. In the West Nankai subduction
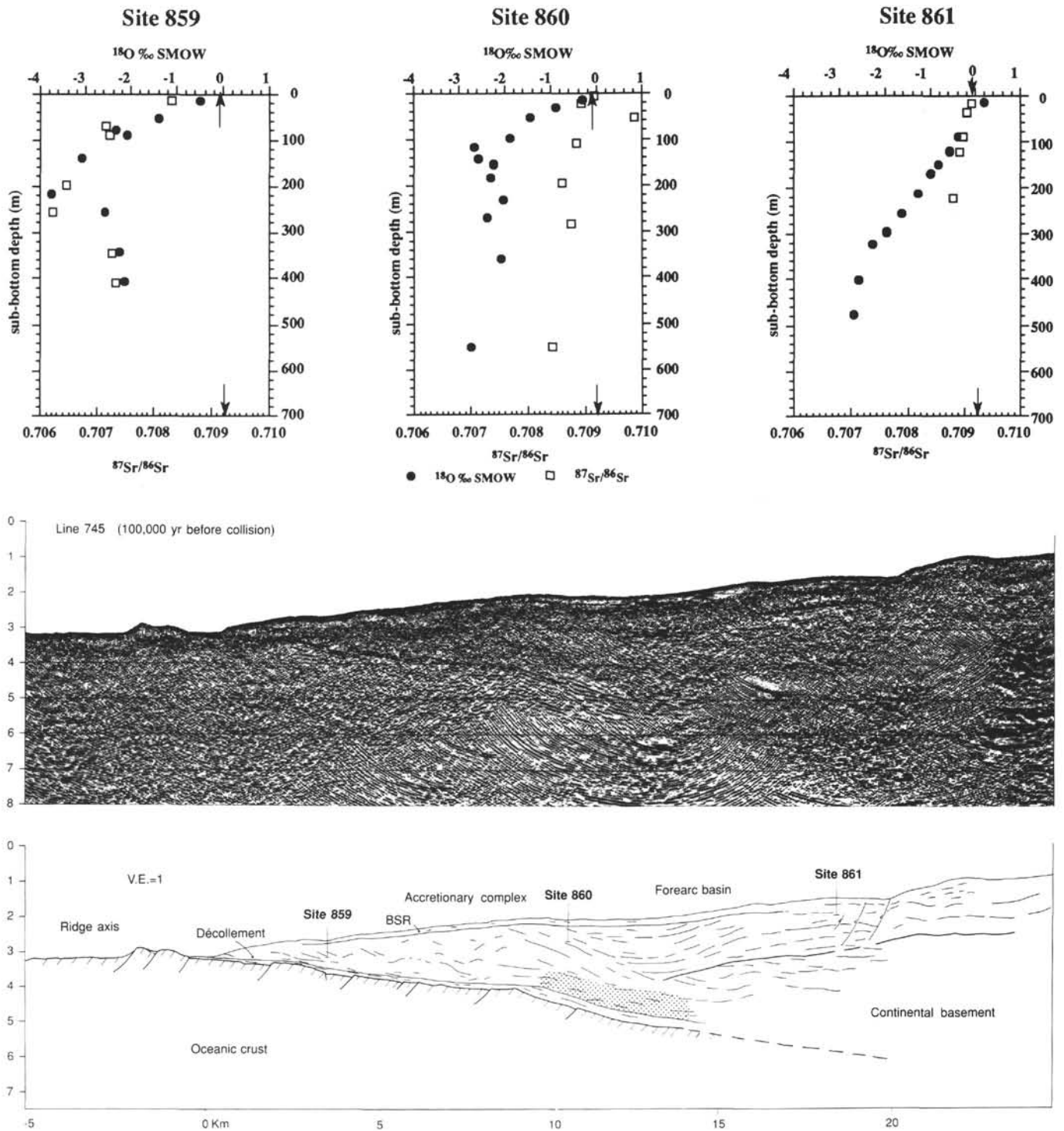
Figure 1. Depth profiles of oxygen and strontium isotope composition of pore fluids from samples recovered in an east–west transect in the pre-ridge collision zone. The minimum at Site 859 (250 mbsf) corresponds to a zone of fluid migration, the isotopic composition indicates that these fluids have been modified by alteration of basalt at low temperature. Contrastingly, the profiles at Site 861 show no evidence for advection of fluids; the distribution is indicative of ion diffusion at this site. The schematic section of the transect from MCS profiles is shown at the bottom (from Behrmann, Lewis, Musgrave, et al., 1992).

zone (Kastner et al., 1992), at New Hebrides Margin site 829 (Martin, 1992), and at Northern Barbados (Vrolijk et al., 1990), smectite to illite transformation at deep burial depth, smectite dewatering, and mixing with meteoric water have all been invoked to explain positive ^{18}O shifts that coincide with Cl concentration decreases. This mechanism cannot be operating at Site 863, because at this site there is an increase in the Cl concentration with depth, which reaches values as high as 614 mM at 687 mbsf (Behrmann, Lewis, Musgrave, et al., 1992).

High temperature basalt-water interaction is called upon to explain the ^{18}O enrichment at Site 863. The observed high values of Ca, low concentrations of Mg, Na, K, and SO_4 and ^{18}O-enrichment are all consistent with experimental basalt-seawater simulations, and with
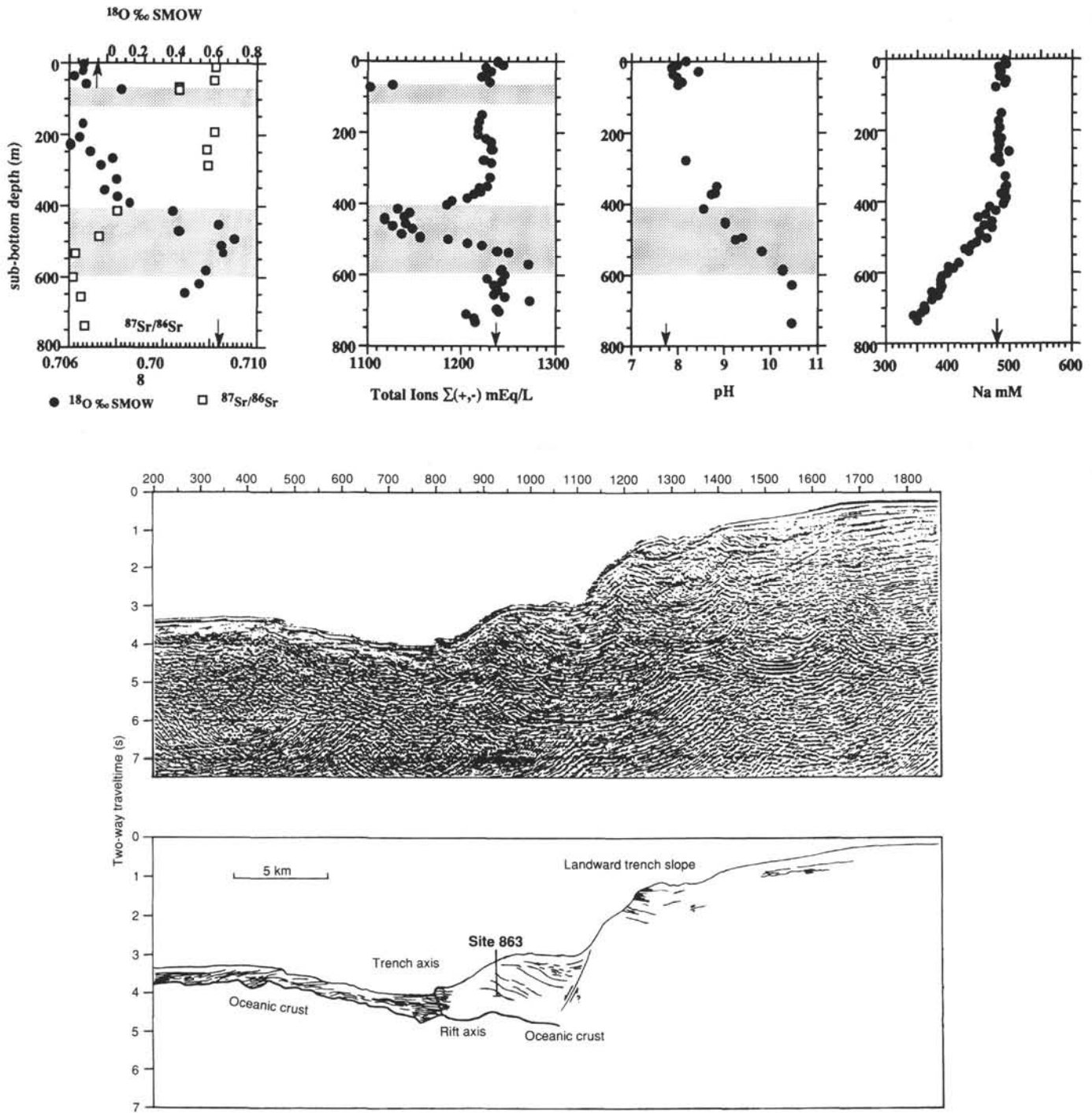
Figure 2. Depth profiles of oxygen and strontium isotope composition, total ions, pH and Na concentration of pore fluids from samples recovered from Site 863, directly above the subducted Chile Ridge spreading center. This distribution is indicative of high-temperature alteration of volcanic materials, likely to be hydrothermal reactions. Shading indicates diagenesis fronts. The schematic section of the transect from MCS profiles is shown at the bottom (from Behrmann, Lewis, Musgrave, et al., 1992).

measured chemical compositions of hydrothermal fluids (Mottl and Holland, 1978; Seyfried and Bischoff, 1979; Edmond et al., 1982). The ^{18}O value in the exiting fluids from hot spring at 21°N EPR is reported as 1.6‰, reflecting basalt equilibrium (Craig et al., 1980). Chloride is concentrated as water is extracted from solution to form hydrated greenschist minerals. In addition, only a small extent of basalt alteration is required to produce the observed ^{18}O change (Fig. 4). The

vertical-bedded sandstone may thus act as a vertical "pipe conduit" tapping deeper fluids altered by basalt-sediment-water interactions.

This hydrothermal fingerprint in the fluid chemistry is also supported by strontium isotope data. The fluids below 400 mbsf have $^{87}Sr/^{86}Sr$ ratio of 0.706, much lower than seawater, indicating almost certainly fresh basalt alteration. Existence of gasoline range thermogenic hydrocarbon below 500 mbsf also requires that the fluids must
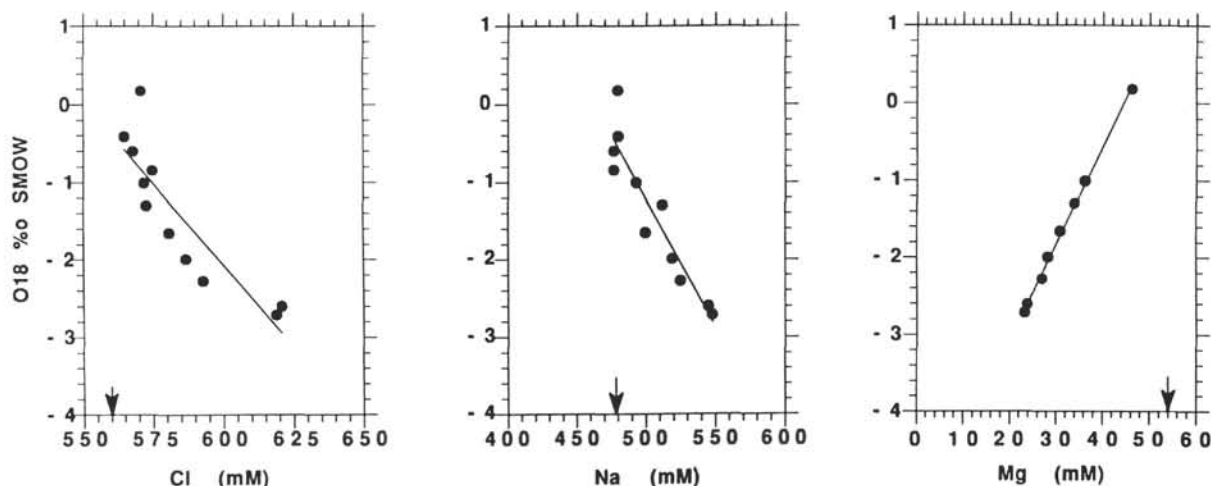
Figure 3. Correlation between the oxygen isotope composition of the pore water and the concentration of dissolved Cl, Na, and Mg at Site 861. These relationships support the conclusion of a diffusion of ions from a depth below 500 mbsf, where the fluids have been modified by conversion of the igneous components of the sediments to authigenic Mg-rich smectites.
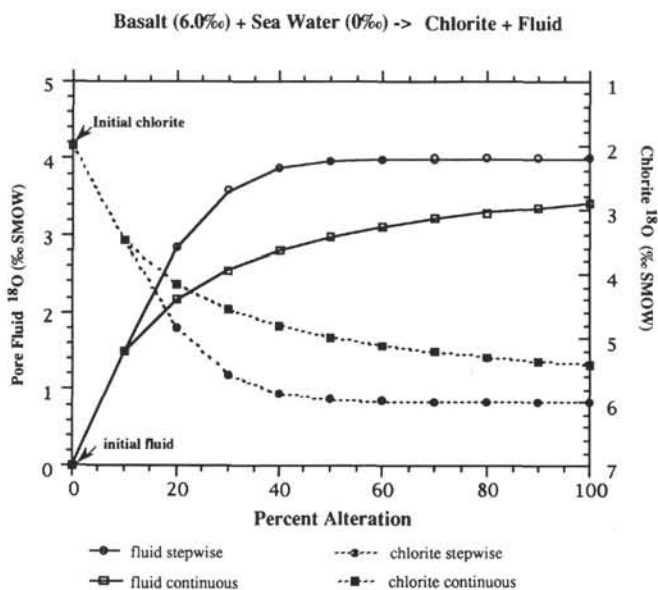

Figure 4. A closed system model calculation to illustrate the effect of high-temperature (200°C) basalt-water interaction on oxygen isotope composition of fluid and chlorite product. Porosity of basalt is taken to be 20%. Curve labeled "continuous" was calculated using a model in which equilibration of the alteration product with the pore fluid was in one continuous batch. Curve labeled "stepwise" was calculated using a model in which alteration proceeded in ten steps. At each step 10% of the solid was altered. The altered solid was then removed from further isotopic equilibration. The pore fluid was equilibrated at each step (after Lawrence et al., 1976).

have experienced temperatures (>150°C) higher than the in-situ temperature regime.

The dramatic increase in ^{18}O is accompanied by a decrease of total ions ("freshening") between 400 to 500 mbsf (Fig. 2). Also, pH, Ca, Mg, and K show discontinuities in this depth interval. One possibility is that hydrothermally influenced water induces a very strong diagenetic front that removes ions from solution. Other evidences supporting this scenario include the following: (1) deconvolutions of tem-

perature logging profiles show a thermal gradient (170°C/km) below 400 mbsf, a value which is twice as high as that from the shallower sequences (Sawyer et al., this volume); and (2) mineralogical changes (cementation front?) have been observed by Prior et al. (this volume). They have shown that smectite and zeolite cements are more extensive deeper than 474 mbsf and always predate the carbonate cement, while above 474 mbsf, carbonate cements are more common.

The secondary mineral phases resulting from basalt-water interaction and calcite veins in the sediment column must be analyzed to reconstruct the fluid isotopic composition and temperature when these minerals formed. These reconstructions may be useful to explain the extremely high pH value below 400 mbsf.

On the other hand, the question of whether there is advection of fluid flow remains. A thrust fault at about 500 mbsf may serve as a conduit for migration of hydrothermally affected fluids. The non-steady state feature of the pore fluid chemistry profile seems to suggest fluid advection. However, one major problem with this fluid advection scenario is the linear Na gradient below 400 mbsf (Fig. 2). This linear Na gradient would require absence of vertical or lateral fluid convection below 400 mbsf. Assuming the Na-gradient is linear below recovery (Behrmann, Lewis, Musgrave, et al., 1992), extrapolation to zero-Na provides a prediction of the basement albitization reaction depth (1500 mbsf) that is consistent with predicted seismic basement (1400 mbsf).

In an attempt to characterize the nature of the hydrothermal fluid, a strontium concentration for the endmember fluid may be estimated, as shown in Figure 5. If assuming that the pore fluids were mixture of hydrothermal fluid and seawater endmembers, a $^{87}Sr/^{86}Sr$ ratio of the high temperature end-member ranging from 0.7028 to 0.7041 as observed for the hydrothermal vent fluids (Von Damm, 1990; Palmer, 1992), with these caveats, a range for the Sr concentration in the hydrothermal fluids was estimated to range from 347 to 2071 μmole/kg. Note that the data deviated from the mixing line (Fig. 5) can be explained by carbonate cementation and therefore are not included in the above estimation. This range is above the upper limit of the observed Sr concentration (335.7 μmole/kg) in hydrothermal vent fluids (Palmer, 1992). We have no further constraints on this estimate unless the $^{87}Sr/^{86}Sr$ ratio of the hydrothermal fluid from the Chile Ridge is measured. Nevertheless, if 0.7041 were taken as the value of $^{87}Sr/^{86}Sr$ ratio for the hydrothermal fluid endmember as measured from 11°–13°N East Pacific Rise (EPR, the closest to Site 863), the endmember Sr concentration would be 347 μmole/kg.
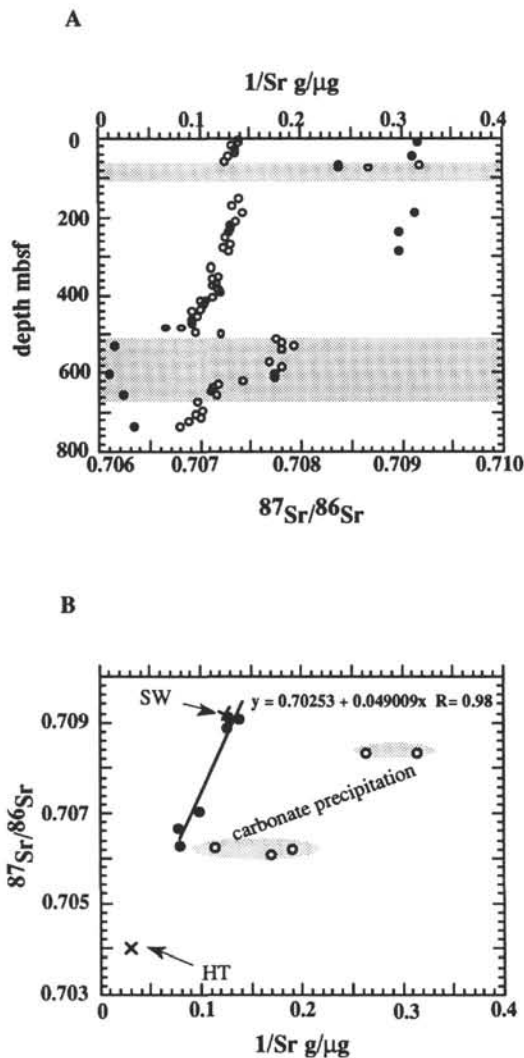
A

B

Figure 5. **A.** Depth profiles of $^{87}Sr/^{86}Sr$ ratios (solid circles) and Sr concentrations (1/Sr, open circles) of pore fluids at Site 863. Shaded areas are the zones of carbonate precipitation. **B.** Distributions of the $^{87}Sr/^{86}Sr$ ratios vs. the inverse of the Sr concentrations at Site 863. Data represented by the solid circles form a mixing line between modern sea water (SW) and an inferred high temperature endmember (HT). The open symbols represent values that have been modified by carbonate precipitation.

If the above estimate were correct, it would imply that a very saline hydrothermal fluid was emitted from Chile Ridge. We may estimate the Cl concentration for Site 863 hydrothermal fluid to be 1.1 mole/kg based on global linear correlation of Sr and square of Cl concentration (Palmer, 1992). Although this value is twice as high as the Cl concentration of seawater, it is only slightly higher than 0.88 mole/kg, which is the maximum observed value for Cl concentration from hydrothermal vent fluids (Palmer, 1992). As Cl is the dominant anion in the fluid phase, the high Cl concentration estimated would essentially require a large amount removal of Cl and major cations in the pore fluids below 400 mbsf and therefore secondary mineral phases enriched in Cl as compared to basalt.

SUMMARY

Oxygen and strontium stable isotopes have been used in conjunction with geochemistry data of pore fluids recovered from four drill sites in the accretionary prism of the Chile Triple Junction to obtain insights on fluid migration and diagenetic processes at these sites. At the pre-ridge collision zone, negative values of ^{18}O SMOW and low values of $^{87}Sr/^{86}Sr$ ratios suggest alteration of volcanic components at low-temperature. At Site 861, fluid interaction is diffusive. At Site 859 and 860, non-steady state depth profiles indicate some lateral fluid movement. The $^{87}Sr/^{86}Sr$ ratio is non-radiogenic (0.706) at the toe of the accretionary prism (Site 859), indicating fresh basalt interaction with fluid.

After ridge subduction (Site 863), the observed positive values of ^{18}O SMOW indicate high temperature alteration of volcanic material. The low $^{87}Sr/^{86}Sr$ ratio almost certainly require this volcanic component to be fresh basalt. A non-steady state situation is reflected in the distribution of dissolved components, data that may be explained as results of dramatic diagenetic reactions in the sediment column. The basal fluids at this site have been affected by the hydrothermal reactions.

ACKNOWLEDGMENTS

REFERENCES*

Bangs, N., Cande, S.C., Lewis, S.D., and Miller, J., 1992. Structural framework of the Chile Margin at the Chile Ridge collision zone. *In* Behrmann, J.H., Lewis, S.D., Musgrave, R.J., et al., *Proc. ODP, Init. Repts.*, 141: College Station, TX (Ocean Drilling Program), 11–21.

Behrmann, J.H., Lewis, S.D., Musgrave, R.J., et al., 1992. *Proc. ODP, Init. Repts.*, 141: College Station, TX (Ocean Drilling Program).

Cande, S.C., Leslie, R.B., Parra, J.C., and Hobart, M., 1987. Interaction between the Chile Ridge and Chile Trench: geophysical and geothermal evidence. *J. Geophys. Res.*, 92:495–520.

Craig, H., Welhan, J.A., Kim, K., Poreda, R., and Lupton, J.E., 1980. Geochemical studies of the 21°N EPR hydrothermal fluids. *Eos*, 61:992.

Edmond, J.M., von Damm, K.L., McDuff, R.E., and Measures, C.I., 1982. Chemistry of hot springs on the East Pacific Rise and their effluent dispersal. *Nature*, 297:187–191.

Elderfield, H., and Gieskes, J.M., 1982. Sr isotopes in interstitial waters of marine sediments from Deep Sea Drilling Project cores. *Nature*, 300:493–497.

Fairbanks, R.G., 1982. The origin of continental shelf and slope water in the New York Bight and Gulf of Mexico: evidence from $H_2^{18}O/H_2^{16}O$ ratio measurements. *J. Geophys. Res.*, 87:5796–5808.

Gieskes, J., Blanc, G., Vrolijk, P., et al., 1989. Hydrogeochemistry in the Barbados accretionary complex: Leg 110 ODP. *Palaeogeogr., Palaeoclimatol., Palaeoecol.*, 71:83–96.

Han, M.W., and Suess, E., 1989. Subduction-induced pore fluid venting and the formation of authigenic carbonates along the Cascadia continental margin: implications for the global Ca-cycle. *Palaeogeogr., Palaeoclimatol., Palaeoecol.*, 71:97–118.

Hesse, R., and Harrison, W.E., 1981. Gas hydrates (clathrates) causing pore-water freshening and oxygen isotope fractionation in deep-water sedimentary sections of terrigenous continental margins. *Earth Planet. Sci. Lett.*, 55:453–462.

Kastner, M., Elderfield H., Jenkins, W.J., Gieskes, J.M., and Gamo, T., 1993. Geochemical and isotopic evidence for fluid flow in the western Nankai subduction zone, Japan. *In* Hill, I.A., Taira, A., Firth, J.V., et al., *Proc. ODP, Sci. Results*, 131: College Station, TX (Ocean Drilling Program), 397–413.

Kastner, M., Elderfield, H., and Martin, J.B., 1991. Fluids in convergent margins: what do we know about their composition, origin, role in diagenesis and importance for oceanic chemical fluxes? *Philos. Trans. R. Soc. London A,* 335:243–259.

Kastner, M., Elderfield, H., Martin, J.B., Suess, E., Kvenvolden, K.A., and Garrison, R.E., 1990. Diagenesis and interstitial-water chemistry at the Peruvian continental margin—major constituents and strontium isotopes. *In* Suess, E., von Huene, R., et al., *Proc. ODP, Sci. Results,* 112: College Station, TX (Ocean Drilling Program), 413–440.

Langseth, M.G., et al., 1988. The role of fluids in sediment accretion, deformation, diagenesis, and metamorphism at subduction zones. *NATO/NSF Workshop, II Ciocco, Italy.*

Lawrence, J.R., 1989. The stable isotope geochemistry of deep-sea pore water. *In* Fritz, P., and Fontes, J.C. (Eds.), *Handbook of Environmental Isotope Geochemistry* (Vol. 3) (2nd ed.): Amsterdam (Elsevier), 317–356.

Lawrence, J.R., Drever, J.I., Anderson, T.F., and Brueckner, H.K., 1979. Importance of alteration of volcanic material in the sediments of Deep Sea Drilling Site 323: chemistry, $^{18}O/^{16}O$ and $^{87}Sr/^{86}Sr$. *Geochim. Cosmochim. Acta,* 43:573–588.

Lawrence, J.R., Gieskes, J., and Anderson, T.F., 1976. Oxygen isotope material balance calculations, Leg 35. *In* Hollister, C.D., Craddock, C., et al., *Init. Repts. DSDP,* 35: Washington (U.S. Govt. Printing Office), 507–512.

Martin, J.B., 1994. Diagenesis and hydrology at the New Hebrides forearc and intra-arc Aoba Basin. *In* Greene, H.G., Collot, J.-Y., Stokking, L.B., et al., *Proc. ODP, Sci. Results,* 134: College Station, TX (Ocean Drilling Program), 109–130.

Mottl, M.J., and Holland, H.D., 1978. Chemical exchange during hydrothermal alteration of basalt by seawater. I. Experimental results for major and minor components of seawater. *Geochim. Cosmochim. Acta,* 42:1103–1115.

Palmer, M.R., 1992. Controls over the chloride concentration of submarine hydrothermal vent fluids: evidence from Sr/Ca and $^{87}Sr/^{86}Sr$ ratios. *Earth Planet. Sci. Lett.,* 109:37–46.

Schrag, D.P., and DePaolo, D.J., 1993. Determination of $\delta^{18}O$ of seawater in the deep ocean during the last glacial maximum. *Paleoceanography,* 8:1–6.

Seyfried, W.E., and Bischoff, J.L., 1979. Low temperature basalt-alteration by sea water: an experimental study at 70°C and 150°C. *Geochim. Cosmochim. Acta,* 43:1937–1947.

Taylor, H.P., Jr., 1990. Oxygen and hydrogen isotope constraints on the deep circulation of surface waters into zones of hydrothermal metamorphism and melting. *In* Norton, D.L., and Bredehoeft, J.D. (Eds.), *The Role of Fluids in Crustal Processes (Studies in Geophysics):* Washington (National Academy Press), 72–95.

Von Damm, K.L., 1990. Seafloor hydrothermal activity: black smoker chemistry and chimneys. *Annu. Rev. Earth Planet. Sci.,* 18:173–204.

von Huene, R., and Scholl, D.W., 1991. Observations at convergent margins concerning sediment subduction, subduction erosion, and the growth of the continental crust. *Rev. Geophys.,* 29:279–316.

Vrolijk, P., Chambers, S.R., Gieskes, J.M., and O'Neil, J.R., 1990. Stable isotope ratios of interstitial fluids from the Northern Barbados Accretionary Prism, ODP Leg 110. *In* Moore, J.C., Mascle, A., et al., *Proc. ODP, Sci. Results,* 110: College Station, TX (Ocean Drilling Program), 189–205.

Yamano, M., Foucher, J.-P., Kinoshita, M., Fisher, A., Hyndman, R.D., and ODP Leg 131 Shipboard Scientific Party, 1992. Heat flow and fluid flow regime in the western Nankai accretionary prism. *Earth Planet. Sci. Lett.,* 109:451–462.